# Highly doped p-type μc-Si through remote inductively coupled plasma assisted chemical vapour deposition (ICP-CVD) for photovoltaic passivation applications

J. W. M. Lim*, Y. Guo, S. Huang, L. Xu, S. Xu
*Plasma Sources and Applications Centre, NIE, Nanyang Technological University*
1 *Nanyang Walk, Singapore 637616*

Institute of Physics (IPS) Meeting 2017

# Introduction

Crystalline silicon based photovoltaic (PV) cells still remains as 1 of the most promising solutions to the global energy crisis by offering a renewable and low cost alternative to conventional fuels, which can be rapidly implemented in industry due to good understanding of silicon based optoelectronic devices driven by the technological revolution. However, **efficiencies of c-Si still remain relatively low** due to either **optical losses** (poor coupling of light into active layers), or **electronic losses** (recombination of photo-generated carriers). In this work, **a remote ICP** facility was used to fabricate **highly doped (~$10^{20}$ cm$^{-3}$) p-type μc-Si thin films** through fragmentation and dissociation of $SiH_4$+$H_2$+$B_2H_6$ feedstocks. The remote configuration of the discharge facility enabled **low damage** of fabricated films typically associated with ICP discharges, while retaining the **uniform discharge characteristics over large areas** with enhanced production of radicals and reactive species. This resulted in **highly crystalline** and highly doped Si films which has huge potential for applications in both c-Si and thin film PV cells as well as other optoelectronic devices.

**The aim of this project was to fabricate highly doped p-type μc-Si thin films through ICP-CVD to serve as a back surface field (BSF) effect passivation layer in PV cells**

# Experimental methods

**1**

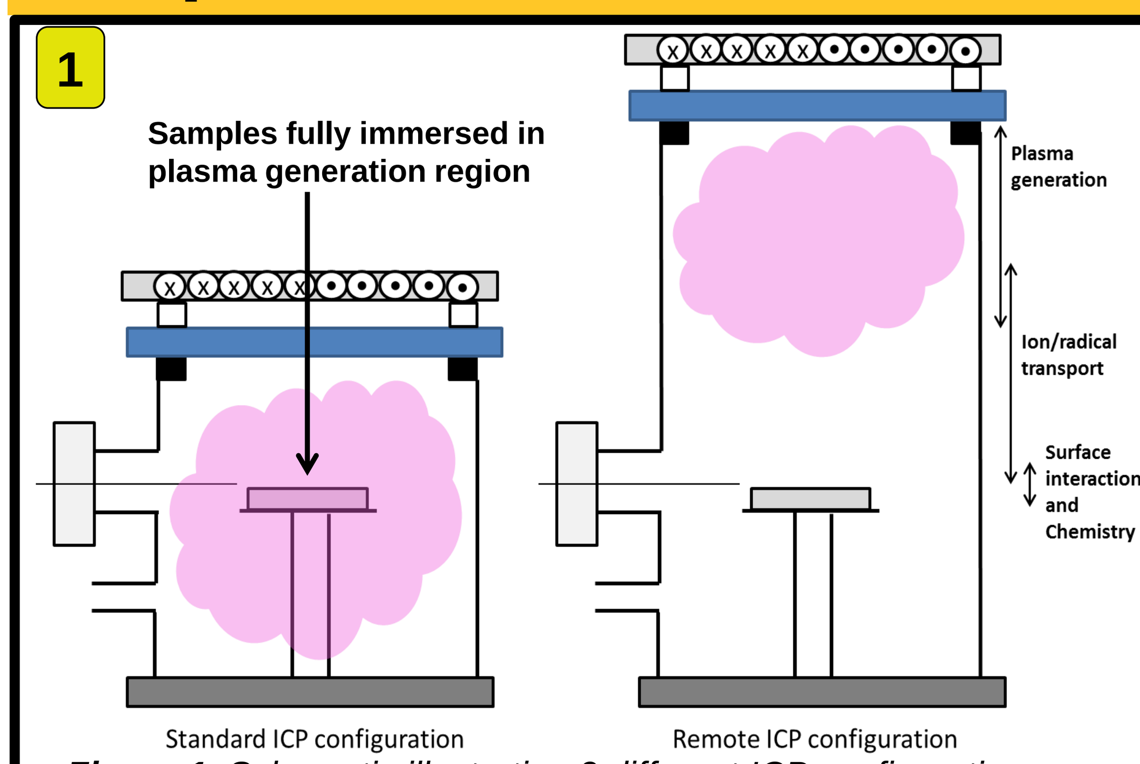


*Figure 1*: *Schematic illustrating 2 different ICP configurations*

A modified **remote ICP reactor** with an **extended height** to the processing stage was used for high quality ICP-CVD. It features

1. High density precursor generation
2. Low ion-bombardment damage
3. In-situ electron heating/lattice recovery
4. Precision control of material properties

**2**

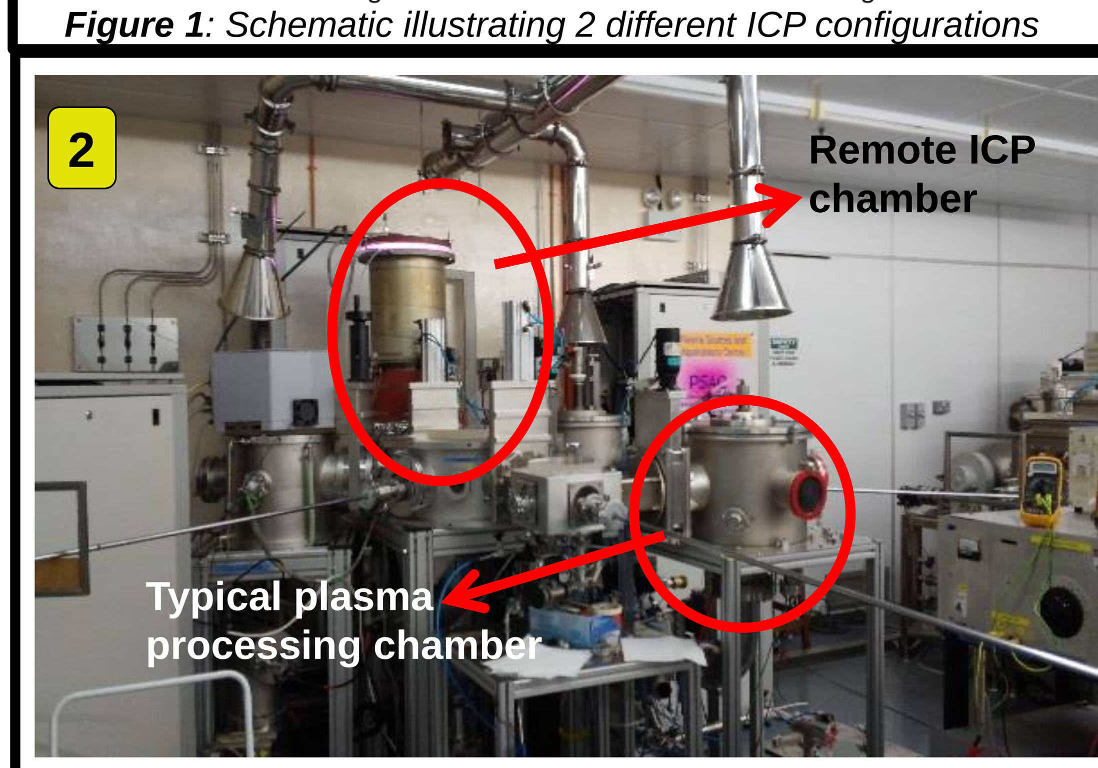


*Figure 2*: *Photo of PSAC's plasma nanofabrication cluster showing the extended height of a remote ICP chamber*

The extended distance from the plasma generation region in the remote configuration enables more pronounced material properties due to segregation of processing into 3 main phases namely

1. Fragmentation and ionization of reactants (Plasma generation)
2. Secondary gas phase reactions/extended ion and radical transport phase
3. Surface interaction and thin film deposition

**3**

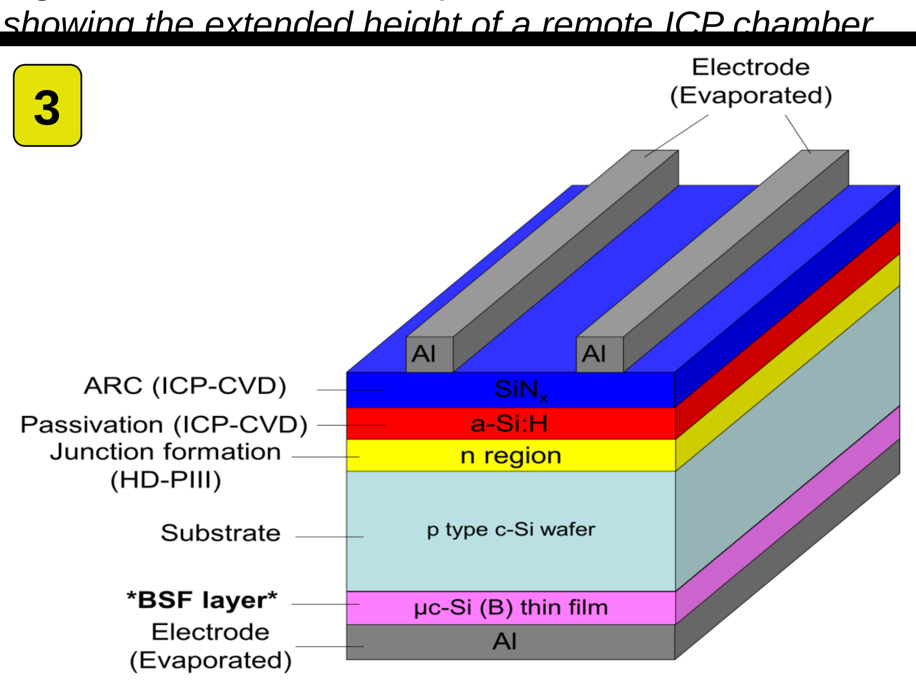


*Figure 3*: *Schematic design of a high efficiency PV cell with BSF passivation layer fabricated at PSAC*

One of the main forms of losses in PV cells is the low lifetime of photo-generated carriers. A BSF passivation layer increases minority carrier lifetime through

1. Provision of a highly doped region at the rear surface
2. Interface between high and low doped region behaves like a "p-n junction" and an electric field forms at the interface
3. Barrier formed to repel minority carrier flux to rear surface
4. Surface recombination velocity greatly reduced
5. Enhanced minority carrier lifetime results in higher $\eta_{eff}$ values

**4**

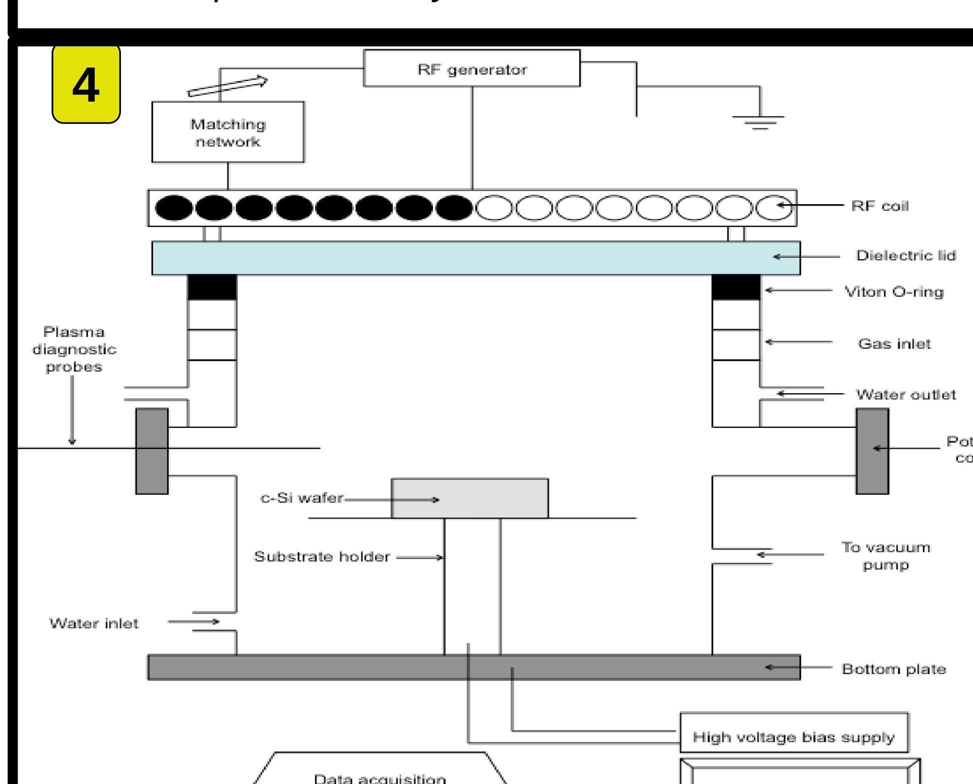


*Figure 4*: *Schematic set-up of the R-ICP reactor used in this work*

A low frequency R-ICP reactor couples 3000 W of RF power through a dielectric lid into a processing chamber filled with $SiH_4$+$H_2$+$B_2H_6$ as feedstocks for film growth

**Experimental conditions**

| Process parameters | |
|---|---|
| RF Power | 3000 W |
| Process time | 15 minutes |
| Substrate temperature | 150 °C |
| Pressure | 2 Pa |
| $SiH_4/H_2$ mass flow ratio | 1:10 |
| $B_2H_6$ flow rate | 1 – 5 sccm |

Large applied RF power and high $H_2$ dilution enhances the crystallinity of thin films

# Experimental results

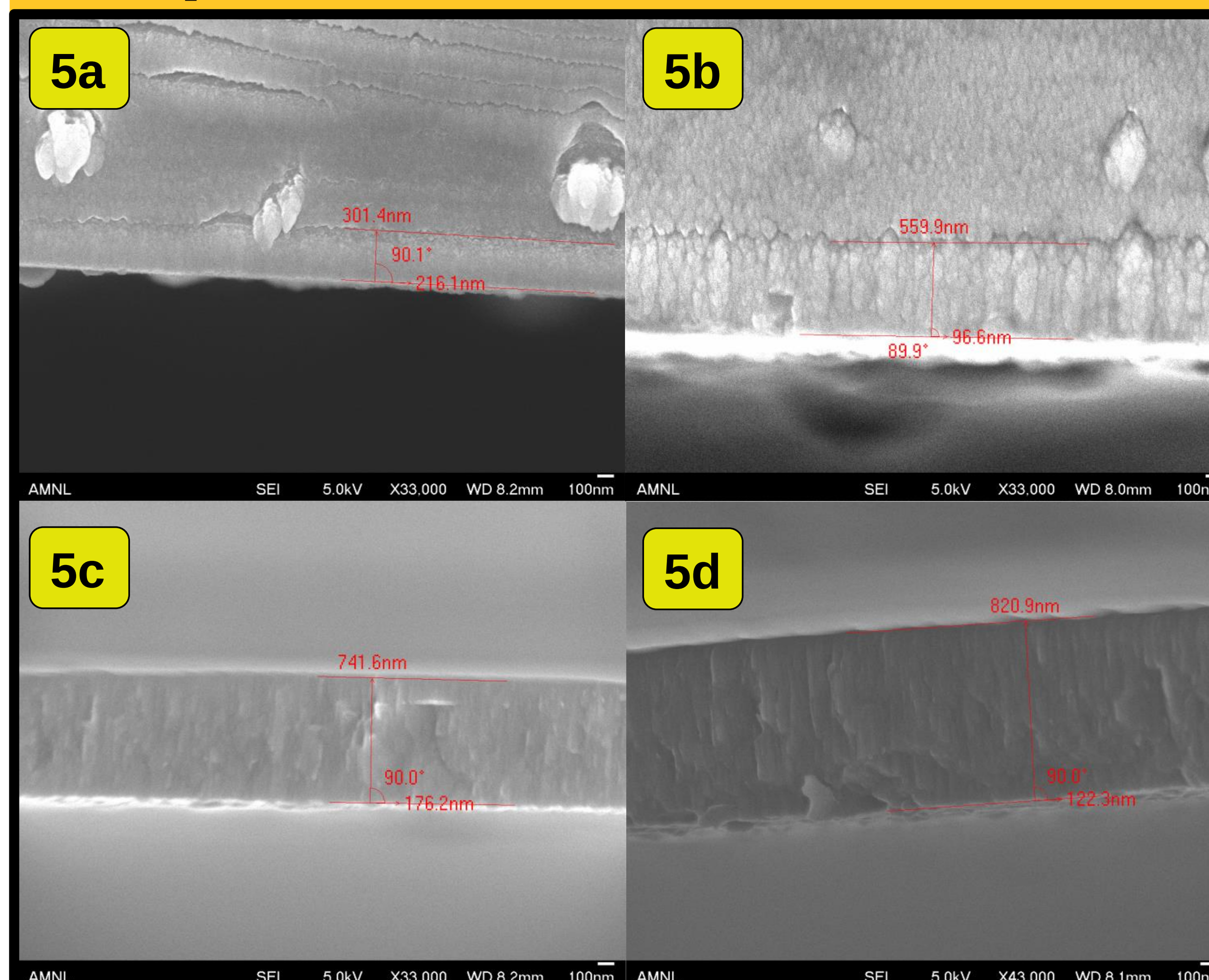


*Figure 5*: *SEM micrographs for thin films deposited with varied $B_2H_6$ flow* ***a.)*** *5 sccm ,* ***b.)*** *4 sccm ,* ***c.)*** *2 sccm ,* ***d.)*** *1 sccm*

Upon lowering of $B_2H_6$ flow in the feedstock recipe, the following are qualitatively determined

1. **Crystallinity** of deposited films **increases**
2. **Deposition rate increases** (thicker films obtained with same deposition time

These observations concur with film growth mechanisms proposed after quantitative determination of dopant incorporation via Hall-effect measurements and Raman spectroscopy

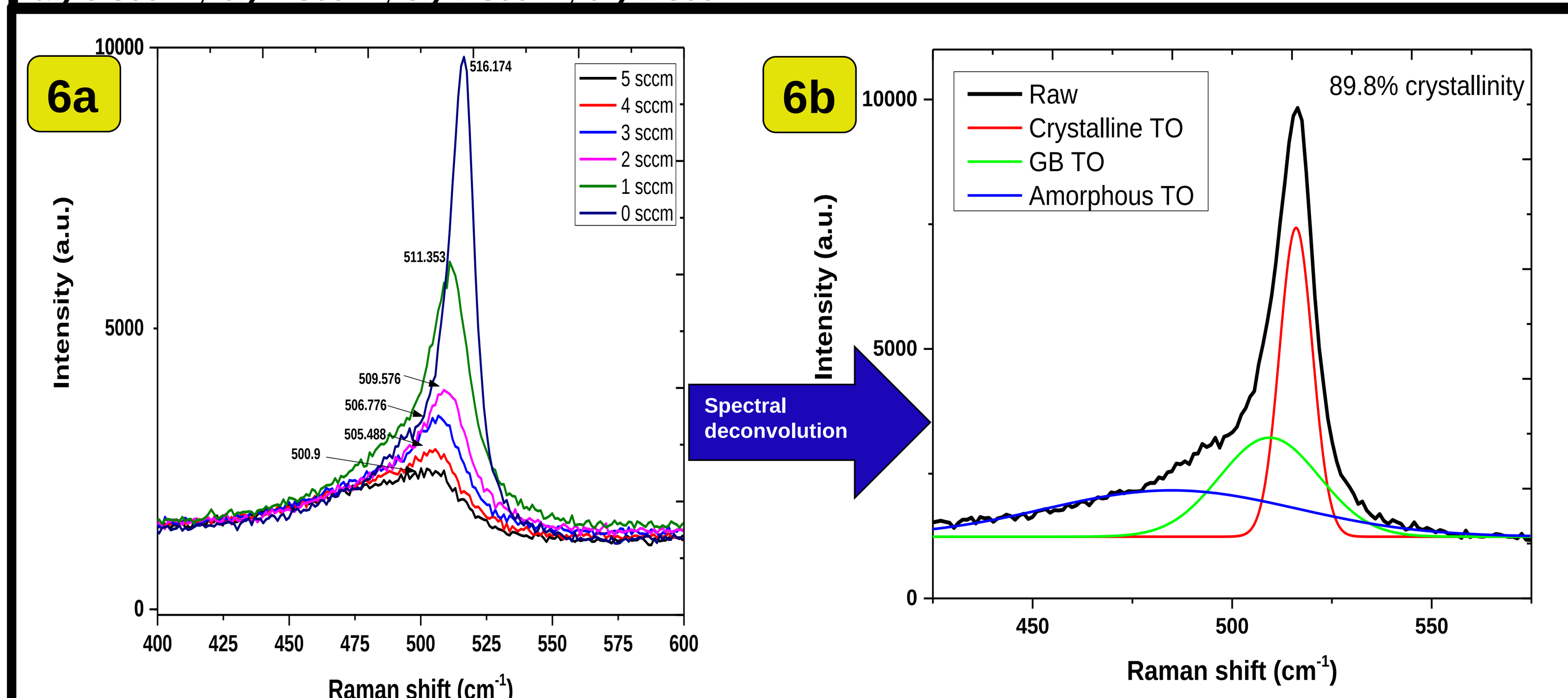


*Figure 6*: ***a.)*** *Raman scattering spectra illustrating redshift of peaks corresponding to crystalline TO modes when $B_2H_6$ flowrate increases* ***b.)*** *Typical spectral deconvolution in determining film crystallinity*

- Crystalline TO modes observed to undergo Raman redshift as $B_2H_6$ flow increases
- Attributed to overall decrease in crystallinity
- Can also be attributed to tensile strain effects due to increased presence of impurities (dopants) → Correlated with HE

- Spectral deconvolution of Raman spectra enables determination of crystallinity

$$\chi_c = \frac{I_{510}+I_{520}}{I_{480}+I_{510}+I_{520}}$$

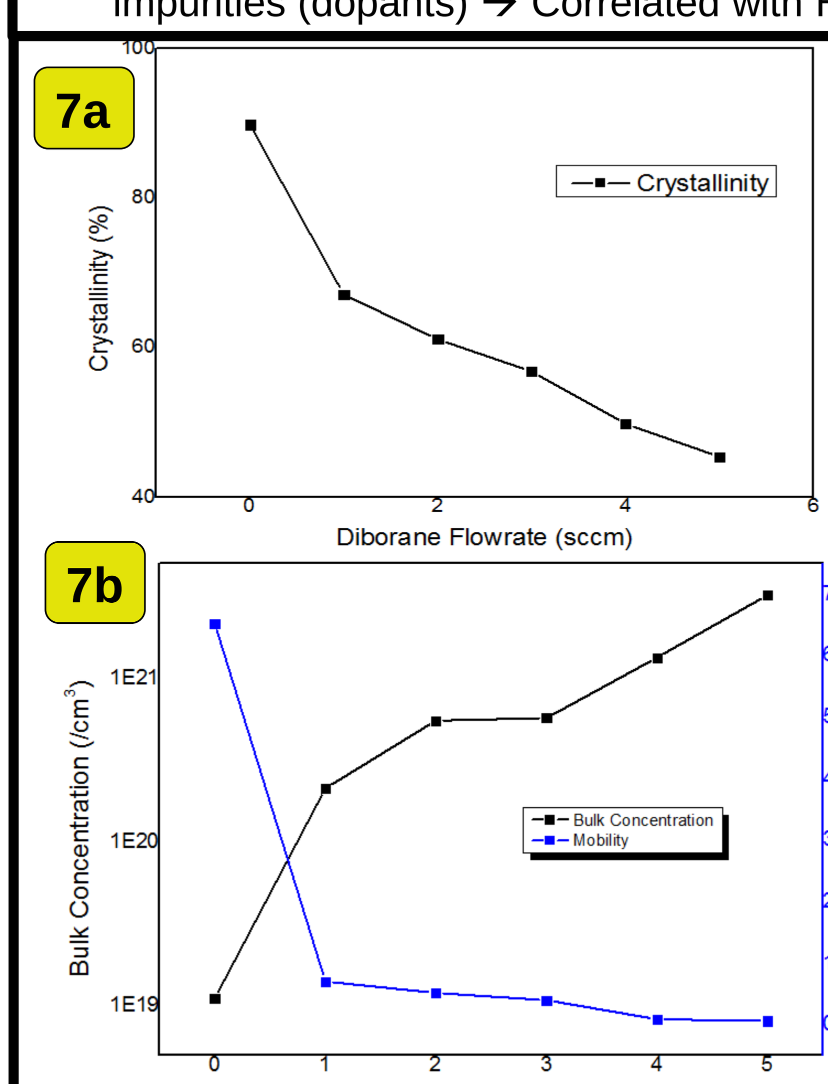


- Films with high crystalline volume fraction, $\chi_c$ (89.8%) were obtained
- $\chi_c$ decreases with $B_2H_6$ flow rate (indicating phase transition – amorphization)
- Phase transition postulated to be due to enhanced incorporation of dopants
- Phonon confinement effects (PCE) due to presence of dopants causes redshift in Raman spectra.
- Redshift also attributed to tensile strain from lattice expansion (increased presence of nanograin boundaries)

- Bulk concentration increases with $B_2H_6$ flow
- Indicates effective boron doping (~$10^{21}$ cm$^{-3}$)
- Dopants also cause disorder in lattice explaining phase transition and redshift in Raman spectra
- Carrier mobility decreases due to scattering of excess carriers with increased doping
- Dark conductivity and photo-response still remains high (device grade), $\sigma_{ph} > 10^5$

*Figure 7*: ***a.)*** *Evolution of film crystallinity as $B_2H_6$ flow increases* ***b.)*** *Evolution of bulk concentration and mobility obtained through hall effect measurements as $B_2H_6$ flow increases*

# Conclusion & further work

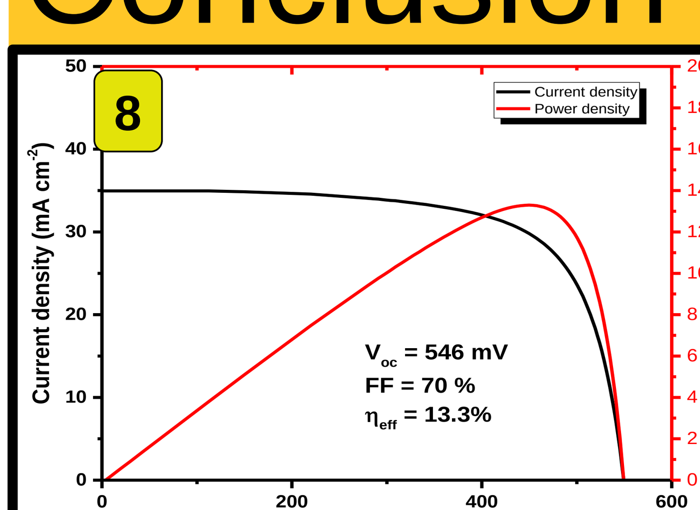


*Figure 8*: *I-V & PV characteristics of high-low junctions formed with μc-Si (B) and a p-type Si substrate*

- Deterministic control of crystalline phase and doping concentration can be achieved through ICP-CVD with $SiH_4$+$H_2$+$B_2H_6$
- High quality "high-low" and p-n junctions demonstrated with fabricated films. Good PV response even without ARC and surface treatment
- Good prospects for TF PV cells/BSF applications
- Work in progress: Incorporation with other plasma processes (texturing, ARC deposition, passivation) in tandem for fabrication of high efficiency PV cells

# References

[1] F. Cerdeira and M. Cardona, "Effect of Carrier Concentration on the Raman Frequencies of Si and Ge," Physical Review B, vol. 5, no. 4, pp. 1440-1454, 1972.
[2] W. Wei, G. Xu, J. Wang and T. Wang, "Raman spectra of intrinsic and doped hydrogenated nanocrystalline silicon films," Vacuum, vol. 81, no. 5, pp. 656-662, 2007.
[3] Z. P. Ling, J. Ge and A. G. A. T. M. R. Stangl, "Detailed Micro Raman Spectroscopy Analysis of Doped Silicon Thin Film Layers and Its Feasibility for Heterojunction Silicon Wafer Solar Cells," Journal of Materials Science and Chemical Engineering, vol. 1, no. 5A, pp. 1-14, 2013.
[4] A. Tabata, J. Nakano, K. Mazaki and K. Fukaya, "Film-thickness dependence of structural and electrical properties of boron-doped hydrogenated microcrystalline silicon prepared by radiofrequency magnetron sputtering," Journal of Non-Crystalline Solids, vol. 356, no. 23-24, pp. 1131-1134, 2010.
[5] P. A. Fedders and D. A. Drabold, "Theory of boron doping in hydrogenated amorphous silicon," PHYSICAL REVIEW B, vol. 56, no. 4, pp. 1864 - 1867, 1997.
[6] N. H. Nickel, P. Lengsfeld and I. Sieber, "Raman spectroscopy of heavily doped polycrystalline silicon thin films," PHYSICAL REVIEW B, vol. 61, no. 23, pp. 15 558 - 15 561, 2000.
[7] Y. Mai, S. Klein, R. Carius, J. Wolff, A. Lambertz, F. Finger and X. Geng, "Microcrystalline silicon solar cells deposited at high rate," Journal of Applied Physics, vol. 97, no. 11, pp. 114913-1 - 114913-12, 2005.

An Institute of NANYANG TECHNOLOGICAL UNIVERSITY

# Highly doped p-type μc-Si through remote inductively coupled plasma assisted chemical vapour deposition (ICP-CVD) for photovoltaic passivation applications

J. W. M. Lim*, Y. Guo, S. Huang, L. Xu, S. Xu
Plasma Sources and Applications Centre, NIE, Nanyang Technological University
1 Nanyang Walk, Singapore 637616

Institute of Physics (IPS) Meeting 2017

# Introduction

Crystalline silicon based photovoltaic (PV) cells still remains as 1 of the most promising solutions to the global energy crisis by offering a renewable and low cost alternative to conventional fuels, which can be rapidly implemented in industry due to good understanding of silicon based optoelectronic devices driven by the technological revolution. However, efficiencies of c-Si still remain relatively low due to either optical losses (poor coupling of light into active layers), or electronic losses (recombination of photo-generated carriers). In this work, a remote ICP facility was used to fabricate highly doped (~$10^{20}$ $cm^{-3}$) p-type μc-Si thin films through fragmentation and dissociation of $SiH_4$+$H_2$+$B_2H_6$ feedstocks. The remote configuration of the discharge facility enabled low damage of fabricated films typically associated with ICP discharges, while retaining the uniform discharge characteristics over large areas with enhanced production of radicals and reactive species. This resulted in highly crystalline and highly doped Si films which has huge potential for applications in both c-Si and thin film PV cells as well as other optoelectronic devices.

**The aim of this project was to fabricate highly doped p-type μc-Si thin films through ICP-CVD to serve as a back surface field (BSF) effect passivation layer in PV cells**

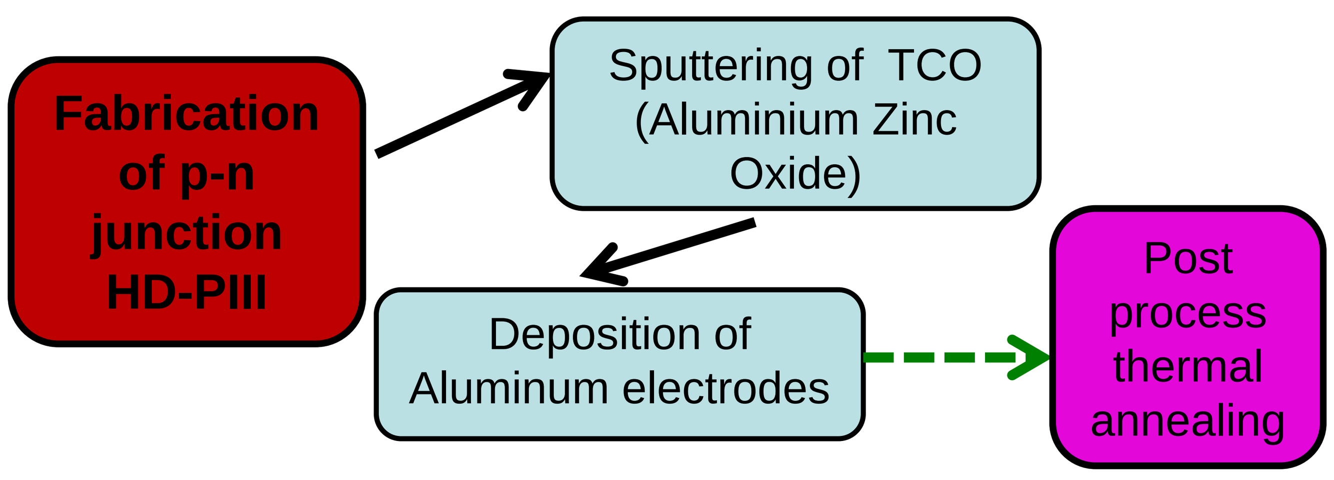


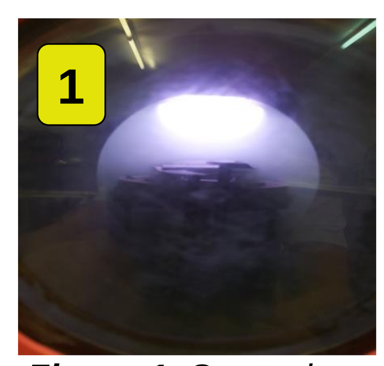

**1**

*Figure 1: Sputtering of a protective TCO layer*

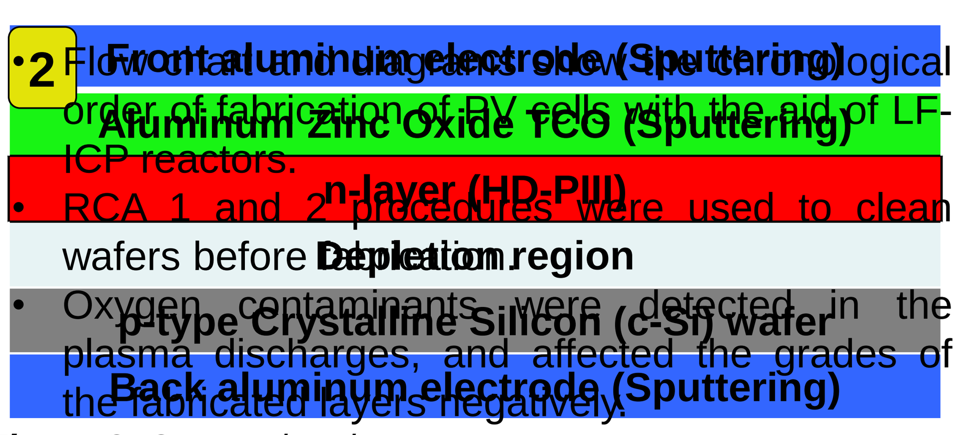


**2**

- Flow chart and diagrams show the chronological order of fabrication of PV cells with the aid of LF-ICP reactors.
- RCA 1 and 2 procedures were used to clean wafers before fabrication.
- Oxygen contaminants were detected in the plasma discharges, and affected the grades of the fabricated layers negatively.

*Figure 2: Conventional PV cell design*
*Figure 3: The LFICP reactor in operation*
*Figure 4: Sample undergoing HD-PIII with Nitrogen plasma discharged in H-mode*

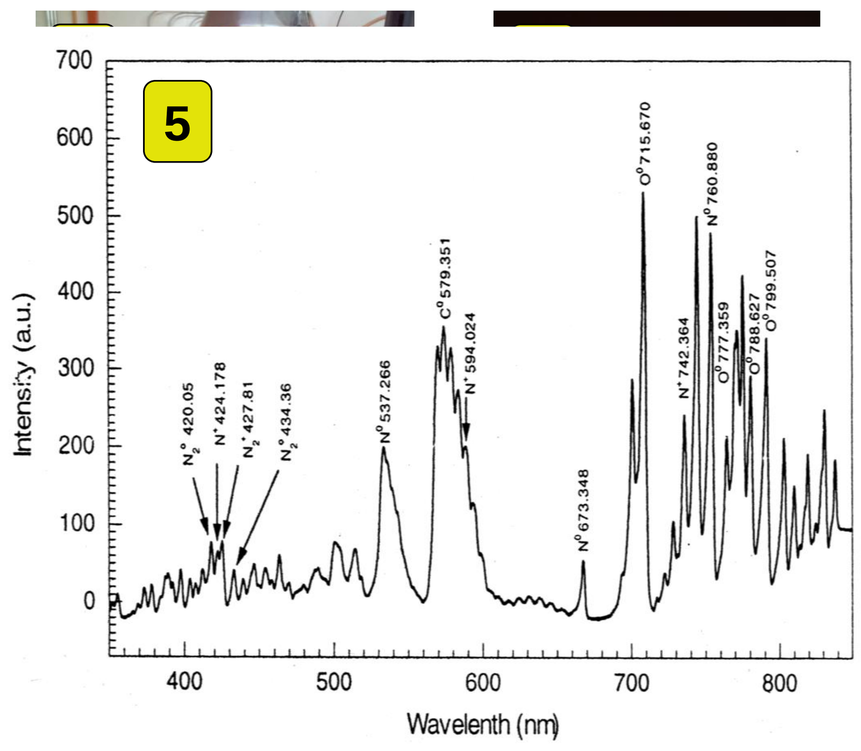


*Figure 5: Optical emission spectra of a plasma discharge showing strong peaks corresponding to oxygen contaminants in a nitrogen plasma discharge*

# Experimental methods

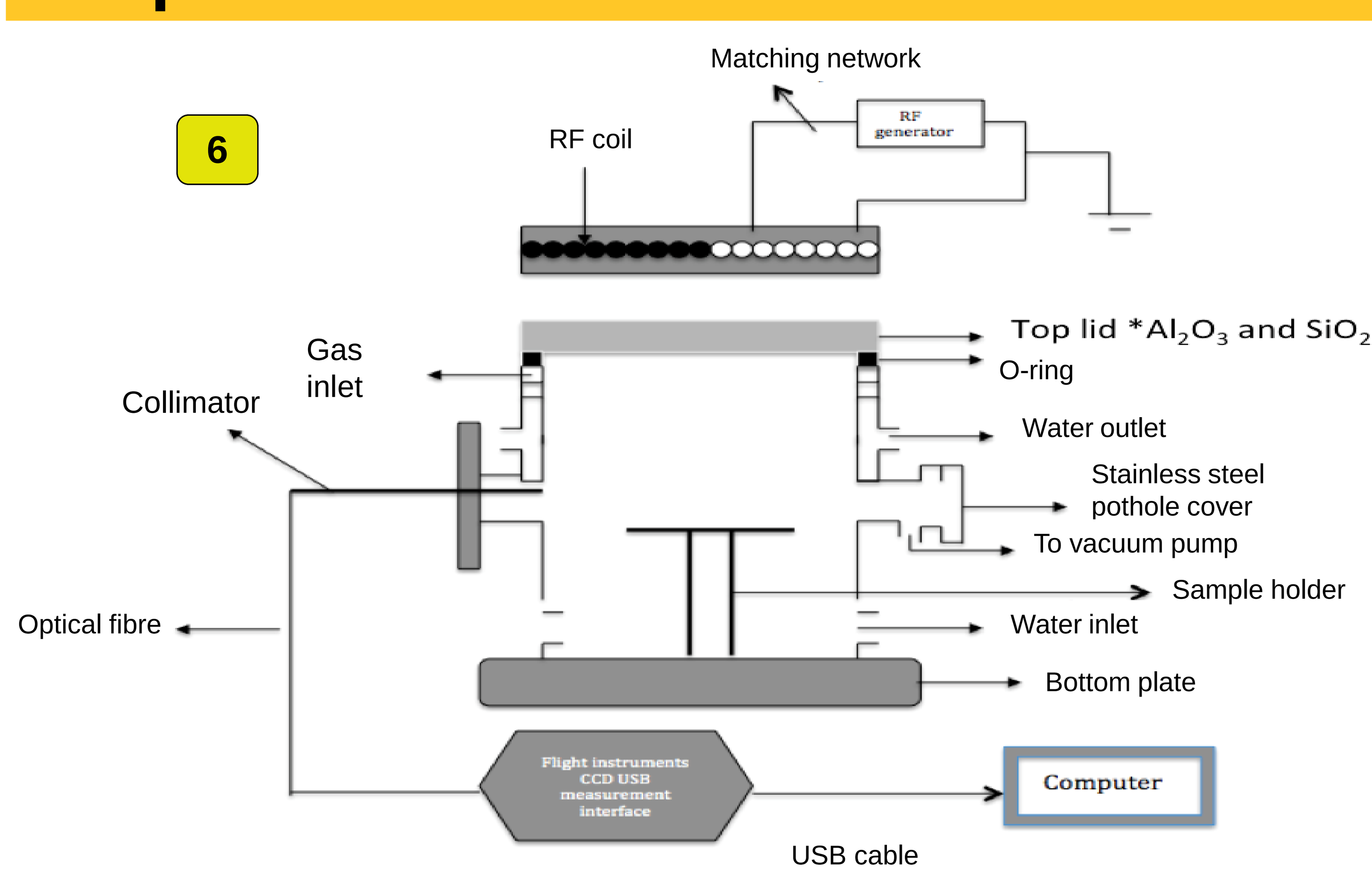


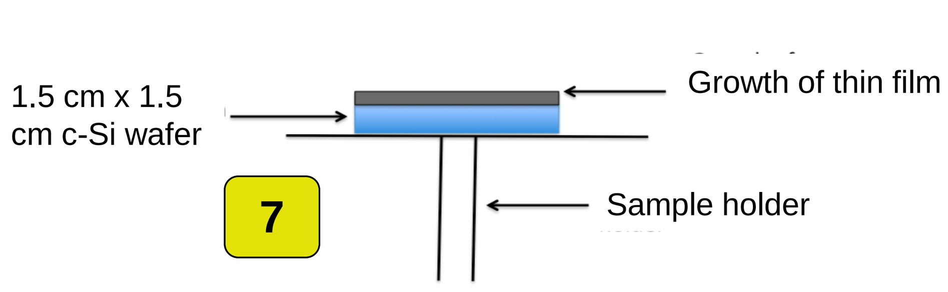


*Figure 6: Schematic set-up of the LF-ICP reactor used in this work*
*Figure 7: Graphical representation of thin film deposition in the LF-ICP reactor (Oxygen contaminant investigation)*

Amorphous hydrogenated silicon was deposited on top of c-Si substrates in a LF-ICP reactor. Experiments were conducted with the conventional quartz ($SiO_2$) lid first, before the lid was swapped out to alumina ($Al_2O_3$). The reactor was evacuated to $10^{-4}$ Pa prior to each experiment with the aid of a turbomolecular pump.

| 8 | Power | Bias | Flow rate | Pressure | Process time | Feedstock gas |
|---|---|---|---|---|---|---|
| | 3.2kW | -750V | 10sccm | 2Pa | 30 minutes | Silane |

Samples were exposed to a high-density silane plasma discharge in electromagnetic (H/bright) mode for deposition of amorphous silicon thin films. The discharge conditions were kept constant for both sets of experiments, with the only variation being the dielectric top lids. The resulting films were characterized with Secondary Ion Mass Spectroscopy (SIMS) and Fourier-transform Infra-red spectrocsopy (FTIR) to reveal the grades of the film and how the lids influence the ability of the reactor to stay free from contaminants.

*Figure 8: Plasma processing parameters which were kept constant for film growth*
*Figure 9: ToF (time of flight) Secondary Ion Mass Spectrometer (SIMS)*
*Figure 10: Fourier-Transform Infra-red spectrometer (FTIR)*


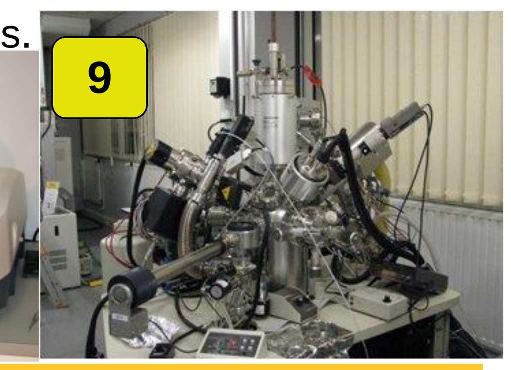


# Experimental results

**Effect of dielectric lids on oxygen content in deposited thin films**

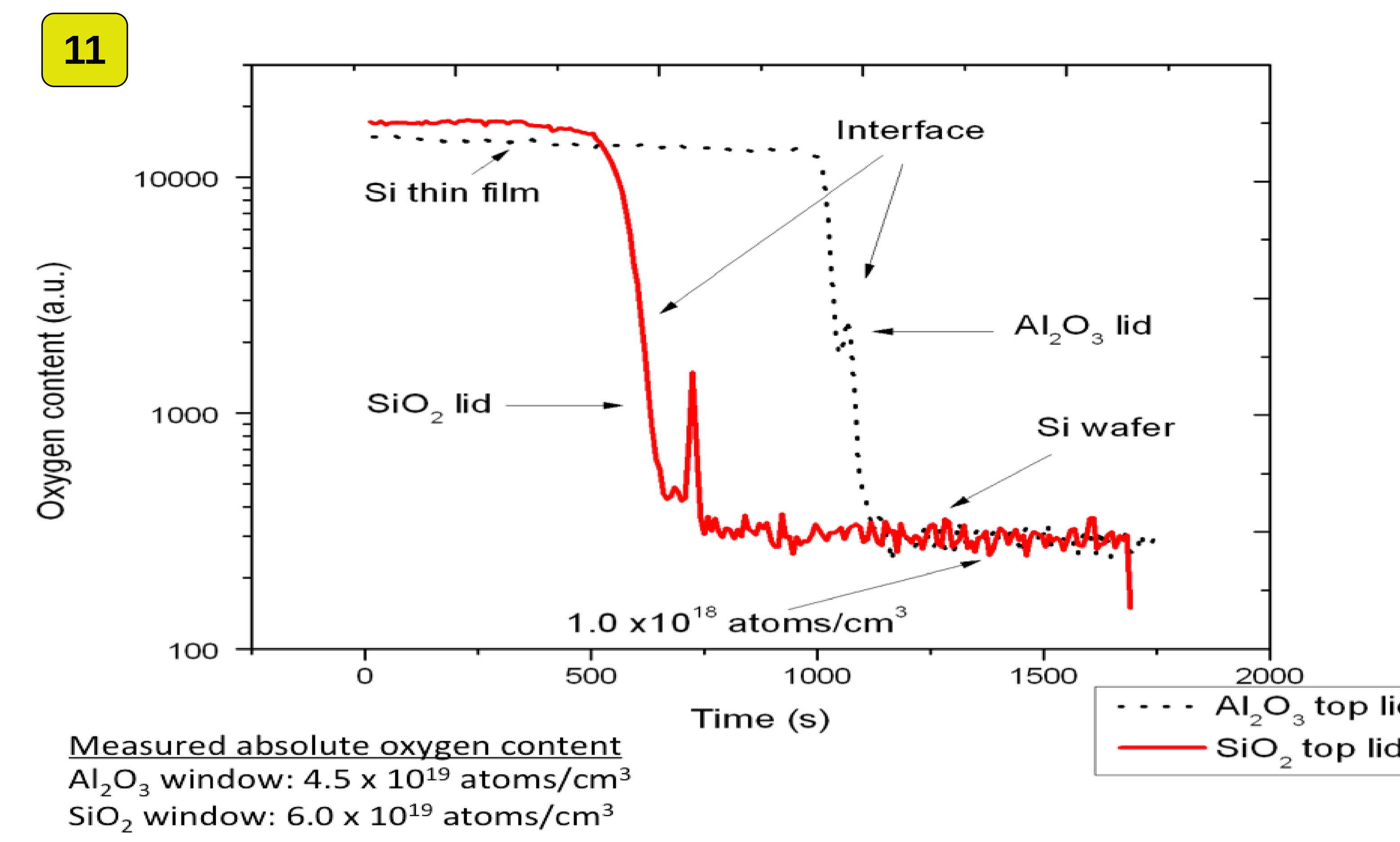


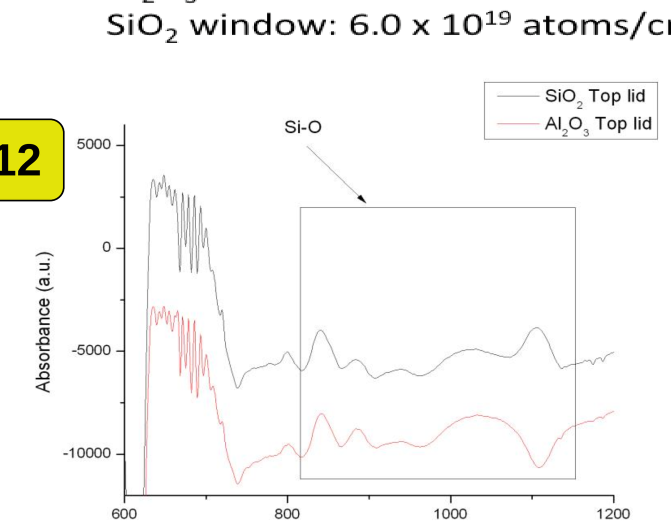


$$\varepsilon_p = 1 - \omega_{pe}^2/[\omega(\omega + i\nu_{eff})]$$

$$P_p = d_t \varepsilon_e$$

$$P_p^H = -\frac{i\omega r^2}{4}\sum_{n=1}^{\infty}\frac{[J_2(p_{1n})I_c\alpha_{1n})^2 \tanh(\gamma_n^p L)}{\cosh^2(\gamma_n^p d)(D_n^p)^2}$$

*Figure 11: SIMS results showing the reduced oxygen content in films deposited with $Al_2O_3$ dielectric lids, and improved deposition rates*
*Figure 12: FTIR results showing the decreased peaks corresponding to Si-O bonding in samples deposited with $Al_2O_3$ lids*

- **Reduction in measured absolute oxygen content in a-Si thin films fabricated with $Al_2O_3$ top lid**
- **Peaks in IR spectra which correspond to Si-O bonding were less pronounced in samples which were fabricated with the $Al_2O_3$ top lid**
- **Deposition rate increased drastically with the $Al_2O_3$ top lid**
- Experimental results concur with theoretical calculations and simulations
- $Al_2O_3$ has a dielectric constant of 9.34 while $SiO_2$ has a dielectric constant of 4.41
- Value for dielectric constant contributes significantly to power delivered to and absorbed by plasma explaining the increase in deposition rate.
- More energy is required to sputter oxygenated species from $Al_2O_3$ as compared to $SiO_2$ accounting for lowered contaminant contents detected in films

# Conclusion & further work

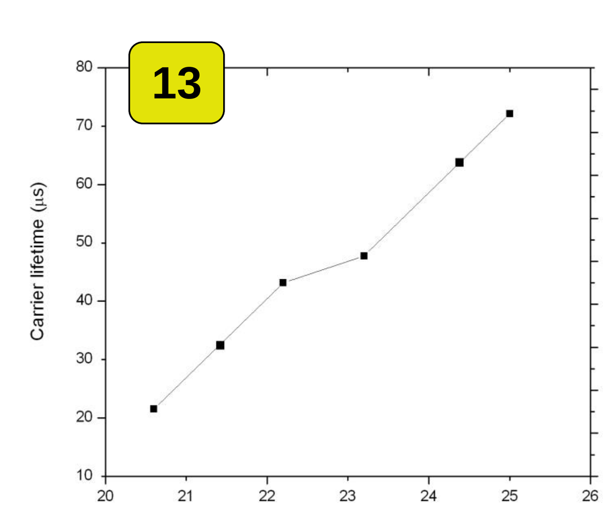


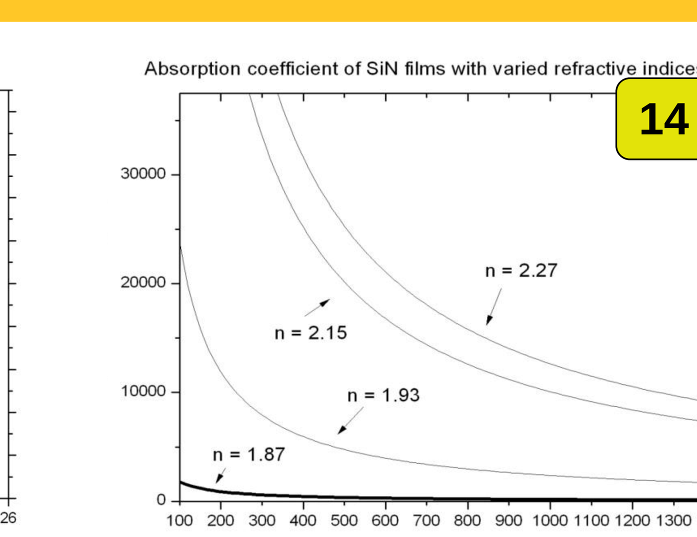


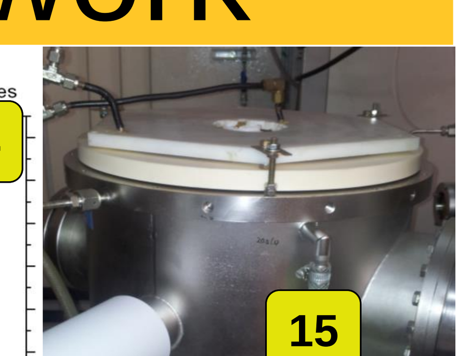


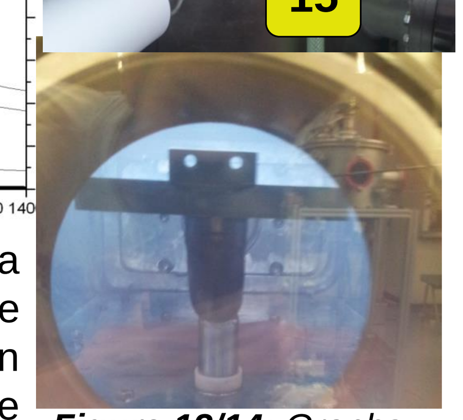

Modification of the conventional quartz dielectric lid to that of alumina has shown promising applications in fabrication of device grade photovoltaic modules in plasma reactors. Apart from reducing oxygen contaminant species, the deposition rate was also seen to increase with the mentioned modifications. High quality contaminant free films are required for high efficiency PV cells. Dry processing in plasma reactors gives added control over the processes by tuning plasma parameters. Further work investigates the passivating qualitites of films by measuring the carrier lifetime. Light management issues are also dealt with in the process.

*Figure 13/14: Graphs showing promising increment in carrier lifetime in films deposited with a-Si*
*Figure 15: Modified CCP reactor texturing c-Si wafers with plasma etching*

# References

1. Anders, A. (2002). From plasma immersion ion implantation to deposition: a historical perspective on principles and trends. *Surface and Coatings Technology , 156*, 3-12.
2. D.A. Horazak, J. B. (1999). Renewables prospects in today's conventional power generation market. *Renewable Energy World , 2* (4), 36.
3. Edward, M., Diaz De La Rubia, T., Erik, S., F., L. J., C., F. J., P., A. R., et al. (2009). A sustainable nuclear fuel cycle based on laser inertial fusion energy. *Fusion Science and Technology , 56*, 547-565.
4. Ostrikov, K., Xu, S., & Lee, S. (2000). Bistability and Hysteresis in Inductively Coupled Plasmas. *Physics Scripta , 62*, 189-193.
5. Ostrikov, K., Xu, S., & Shafiul Azam, A. (2002). Optical emission characteristics and mode transitions in low-frequency inductively coupled plasmas. *Journal of Vacuum Science & Technology A: Vacuum, Surfaces, and Films , 20* (1), 251-264.
6. S.Xu, K.N.Ostrikov, Luo, W., & Lee, S. (2000). Hysteresis and mode transitions in a low-frequency inductively coupled plasma. *Journal of Vacuum Science and Technology , 18*, 2185-2197.
6. Azam, A. S. (2000). *Optical emission spectroscopy studies of a high density, low frequency inductively coupled RF plasma source.* Singapore.
7. Philipps-UniTersitä̀t. (1998). Semiconductor processing by plasma immersion ion implantation. *Materials Science and Engineering* , 258-268.
8. Khanh, N., Pinter, I., Dusco, C., Adam, M., Szilagyi, E., Barsony, I., et al. (1996). Ion beam analysis of plasma immersion implanted silicon for solar cell fabrication. *Nuclear Instruments and Methods in Physics Research B* , 259-262.
9. Bogaerts, A., Neyts, E., Gijbels, R., & Mullen, J. c. (2001). Gas discharge plasmas and their applications. *Spectrochemica Acta Part B , 57*, 609-658.
10. Martin A. Green, K. E. (2009). Solar cell efficiency tables (version 35). *Progress in Photovoltaics: Research and Applications , 18*, 144-150.

natural sciences and science education academic group

An Institute of NANYANG TECHNOLOGICAL UNIVERSITY